UNCLASSIFIED

AD NUMBER
AD525790
CLASSIFICATION CHANGES
TO: **UNCLASSIFIED**
FROM: **SECRET**
LIMITATION CHANGES
TO: **Approved for public release; distribution is unlimited.**
FROM: **Distribution authorized to U.S. Gov't. agencies only; Test and Evaluation; 11 MAY 1973. Other requests shall be referred to Electronic Systems Division, ATTN: ESD-DR-2, Hanscom AFB, MA 01730.**
AUTHORITY
DARPA ltr dtd 26 Oct 1983; DARPA ltr dtd 26 Oct 1983

THIS PAGE IS UNCLASSIFIED

AD- 525790

SECURITY REMARKING REQUIREMENTS

DOD 5200.1-R, DEC 78

REVIEW ON 02 MAY 93

SECURITY

MARKING

The classified or limited status of this report applies to each page, unless otherwise marked.
Separate page printouts MUST be marked accordingly.

ESD-TR-73-99

Secret

Technical Note 1973-19

J. O. Dimmock

IR Satellite Surveillance

(Title UNCLASSIFIED)

2 May 1973

Prepared for the Advanced Research Projects Agency
under Electronic Systems Division Contract F19628-73-C-0002 by

Lincoln Laboratory

MASSACHUSETTS INSTITUTE OF TECHNOLOGY

LEXINGTON, MASSACHUSETTS

Secret

Distribution limited to U.S. Government agencies only; test and evaluation; 11 May 1973. Other requests for this document must be referred to ESD-DR-2.

This document comprises 26 pages. No. 26 of 80 copies.

MASSACHUSETTS INSTITUTE OF TECHNOLOGY

LINCOLN LABORATORY

IR SATELLITE SURVEILLANCE

(Title UNCLASSIFIED)

J. O. DIMMOCK

Group 52

TECHNICAL NOTE 1973-19

2 MAY 1973

"NATIONAL SECURITY INFORMATION"

"Unauthorized Disclosure Subject to Criminal Sanctions"

This docu[redacted] contain[redacted]ation affecting[redacted] national de[redacted] of the [redacted] State[redacted]thin [redacted] meaning [redacted]pionage [redacted] [redacted] Sec[redacted]ons 793 [redacted] 794. [redacted] of its contents in any ma[redacted] an unautho[redacted] person is prohibited by law.

EXCLUDED FROM GDS
(DD Form 254 GP 3)

Distribution limited to U.S. Government agencies only; test and evaluation; 11 May 1973. Other requests for this document must be referred to ESD-DR-2.

DDC CONTROL NO 31279

L. G. Hanscom Field
Bedford, Mass. 01730

LEXINGTON MASSACHUSETTS

The work reported in this document was performed at Lincoln Laboratory, a center for research operated by Massachusetts Institute of Technology. This work was sponsored by the Advanced Research Projects Agency of the Department of Defense under Air Force Contract F19628-73-C-0002 (ARPA Order 600).

ABSTRACT

(U) A calculation and a comparison is made between the capabilities of a linear array of infrared detectors and those of an infrared vidicon for detecting high-altitude satellites from a satellite sensor platform. It is shown that far smaller optics diameter is required for the vidicon sensor to achieve the same range as the linear array or alternatively the vidicon range is far greater.

Accepted for the Air Force
Joseph J. Whelan, USAF
Acting Chief, Lincoln Laboratory Liaison Office

IR SATELLITE SURVEILLANCE (U)

I. INTRODUCTION

(S) In this report we consider the detection of high-altitude satellites using their thermally emitted infrared radiation. The sensor is assumed mounted on a search satellite, and two different sensor systems are considered. One system consists of a linear array of individual detectors and the other consists of an infrared vidicon. Considerable analysis of these two systems is contained in the report[1] of an earlier study. As in the case of the earlier study it is obvious that a considerable reduction in the size, and consequently in the weight and cost of the sensor system can be realized by the development and employment of a sensitive, low-background IR vidicon.

(S) The sensor establishes a "tight fence" in that every satellite at greater than synchronous altitude must pass through the sensor field-of-view four times per relative sensor-target orbit. This gives approximately four "hits" per 24 hours on all targets above this altitude. It is anticipated, however, that much, and perhaps most, of the time will be spent in a tracking mode, obtaining orbital information on targets detected.

Search Pattern

(S) The model search pattern is shown in Fig. 1. The search satellite is assumed to be in earth synchronous orbit at 36,000-km altitude as was the case for the high orbit scheme considered in the earlier study. The orbital period is 24 hours and the scan rate is such that any satellite at 3-times-synchronous altitude or beyond cannot pass through the pattern without being in the field-of-view of the sensor at least twice. The required scan rate for this is 3.5 str/hour. In the analysis below we consider a scan rate requirement of 3.5 str/hour for the linear

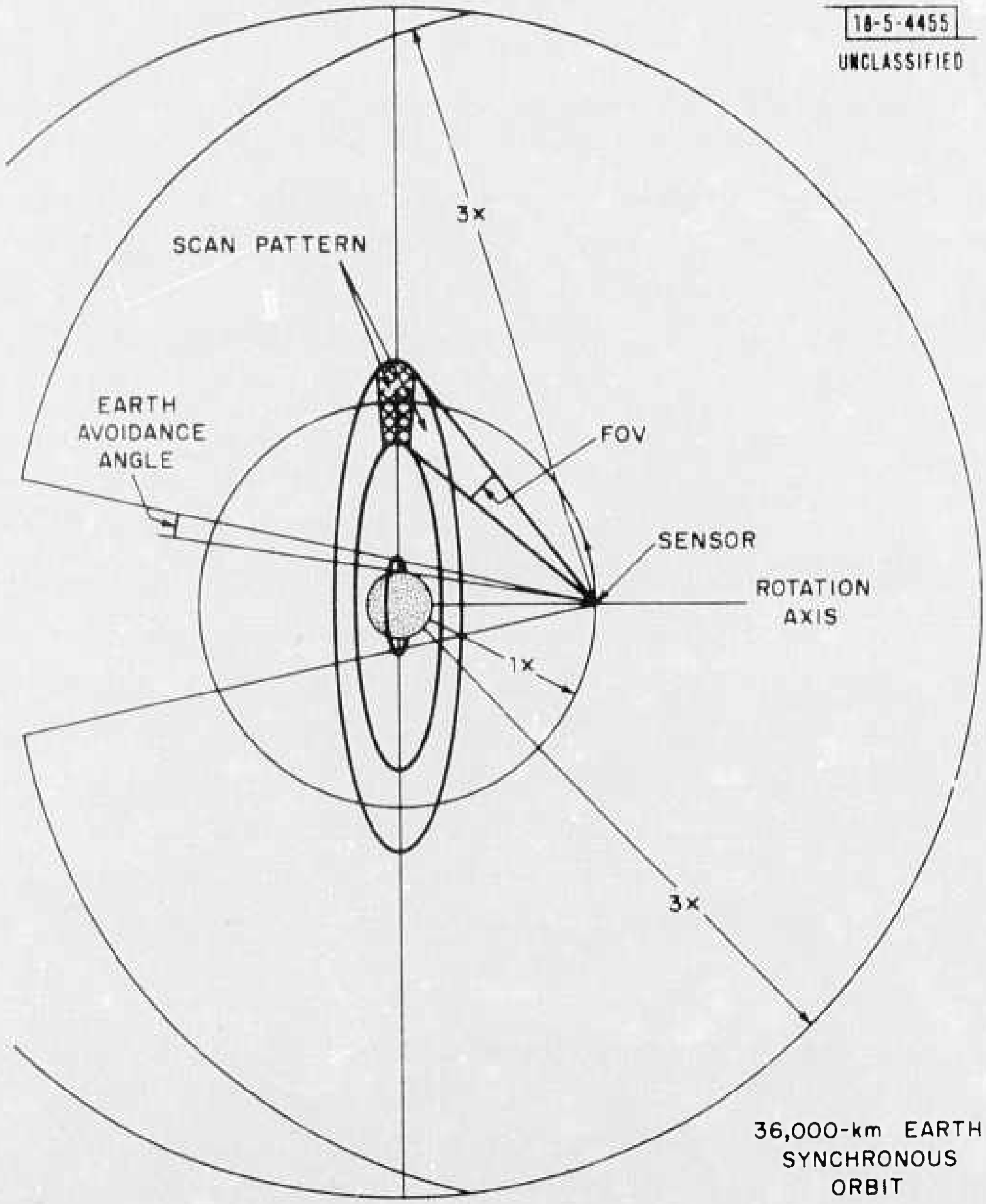

Fig. 1. IR satellite surveillance scan pattern. (U)

array and 4.0 str/hour for the vidicon since part of the vidicon search time will be lost as the sensor is stepped to the next field-of-view.

(U) In order to generate the scan pattern the search satellite rotates about an axis directed approximately toward the center of the earth. In the designs considered below the linear array sensor rotates 360° once every 23 minutes and readjusts its rotation axis by 5.7° toward the earth center and repeats the scan overlapping half of the previous scan. The vidicon sensor rotates in a step pattern of 56 steps, 6.5° each, covering 360° once every 13 minutes (11.6 seconds/frame plus 2.3 seconds for each step = 14 seconds/picture). The pattern is then repeated with registration on the previous frames and the signals from the two corresponding frames compared to observe relative satellite motion. At the end of 26 minutes the rotation axis is readjusted 6.5° toward earth center and the process repeated.

Target Models

(S) The infrared and visible target model spectral signatures are shown in Fig. 2. Curves are given in photons/sec μm for targets A, B, and C/10 for convenience. The curve labeled C/10 represents one tenth the signature of assumed target C, ($10m^2$, 300°K, $\varepsilon=1$, $\gamma=0.5$) and is equal to that of the target model assumed in the earlier study. The 8-22μm region shown cross-hatched contains most of the infrared target irradiance and can be covered by the Si:As detector material discussed in the earlier study report. The target irradiance in this region for three targets is

$$Q_s = 8.2\times10^{21} \text{ photons/sec} \quad \text{(target A)}$$
$$Q_s = 1.44\times10^{22} \text{ photons/sec} \quad \text{(target B)} \qquad (1)$$

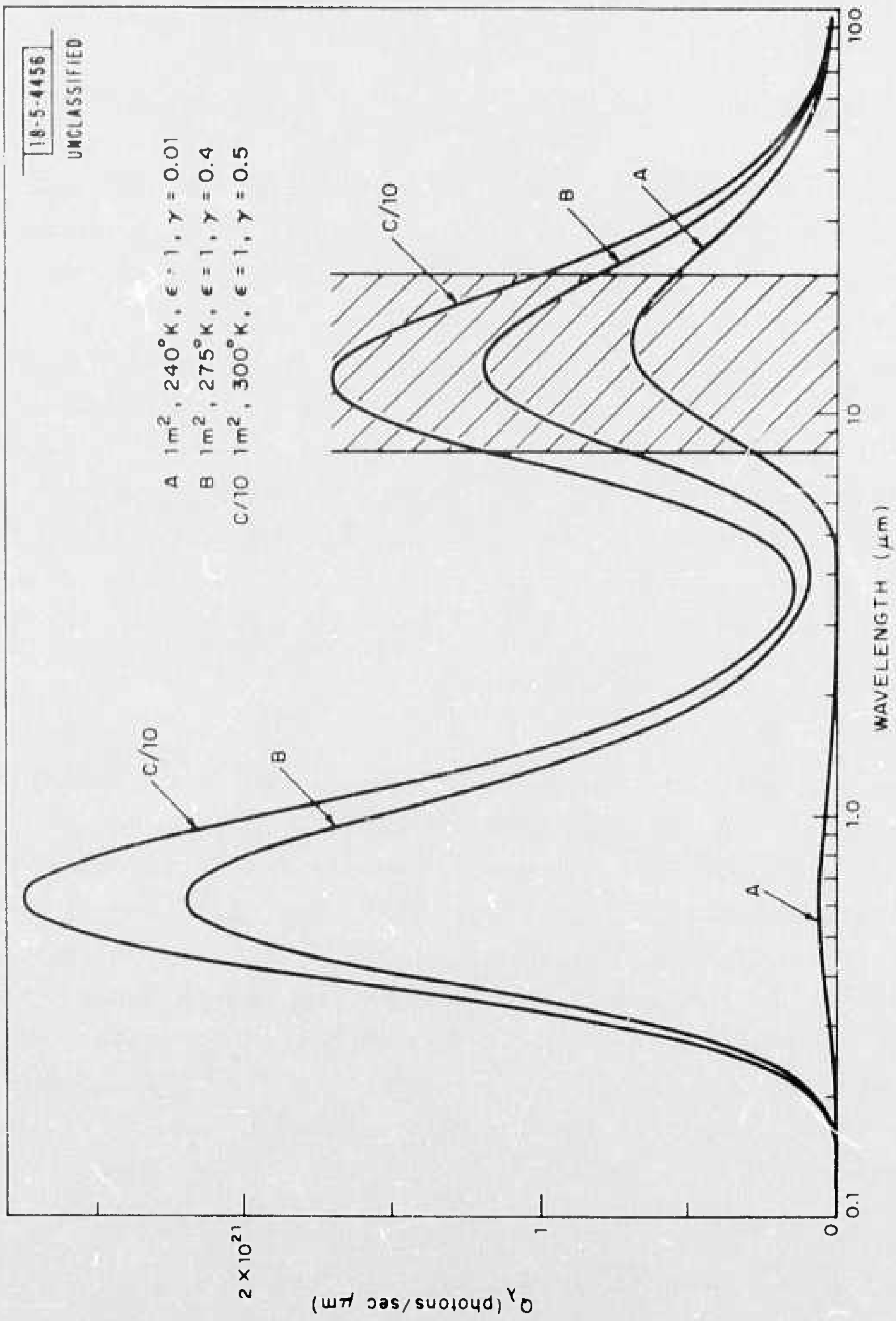

Fig. 2. IR and visible target model signatures. (U)

$Q_s = 1.98 \times 10^{23}$ photons/sec (target C)

We use this band in the present study instead of the 8-14μm band used before because of the lower target temperatures of targets, A and B. In the following analysis we will consider only target A as its signature is not much different from that of target B, and target C presents no real challenge to the system.

Backgrounds

(U) The point source stellar and diffuse cosmic background levels can be roughly obtained as they were in the earlier study. From the infrared rocket-borne measurements of Soifer, Houck and Harwit[2] we obtain a background photon flux for the 8-22μm region of

$$Q_B = 2.42 \times 10^{10} \text{ photons/sec cm}^2 \quad (2)$$

at an ecliptic elevation of ± 15° and an elongation from the sun of 160°. This appears to be due to zodiacal radiation and will be greater at lower elevation angles and less elongation, and less at higher elevation angles. It probably represents a reasonably good average value.

(S) The number of stars per square degree with 8-22μm radiance greater a given quantity has been extrapolated from the results of Hi-Star measurements reported by Price and Walker.[3] Compiling their 8-14μm and 16-22μm data the following relation is obtained for angles >5° off the galactic plane:

$$N = 3750\ Q^{-1.05} \text{stars/deg}^2 \text{ (Q in photons/sec cm}^2\text{)} \quad (3)$$

for the 8-22μm region. Their data is obtained in the region $Q>5000$ photons/sec cm^2 whereas our region of interest is between $5 \leq Q \leq 500$ photons/sec cm^2 which represents up to three orders of magnitude extrapolation from their data. This extrapolation is dubious at best, and is used simply for lack of something better.

(U) Since the target irradiance at the sensor can be obtained from the target radiances given in Eq. (3) by dividing by πR^2, where R is the sensor-to-target range, the number of stars per deg^2 with irradiance equal to or greater than that of the various targets can be obtained as a function of R. A plot of these star densities is given in Fig. 3 for Targets A and C/10.

Analysis

(U) The range-sensitivity relation can be obtained following the analysis of Appendix A in the report of the earlier study.[1] For the background-limited linear array, from Eq. A-44 of the earlier study report we have

$$R^2 = \frac{Q_s}{4\,(SNR)} \quad D\left(\frac{T_o}{Q_B}\, 2n\eta\dot{\Omega}^{-1}\right)^{1/2} \tag{4}$$

where R is the sensor-to-target range, Q_s is the signal flux given by Eq. (3) ($Q_s = W_{\Delta\lambda}A/h\nu$ in Eq. A-44), SNR is the signal-to-noise ratio, D is the optics diameter, T_o is the optics transmission, Q_B is the background flux, n is the number of detector elements, η is their quantum efficiency and $\dot{\Omega}$ is the scan rate. For a linear array n can be related to the angular field-of-view of the sensor, Ω_{FOV}, and the instantaneous field-of-view of the individual detectors, ω_{FOV} by

$$n = \Omega_{FOV}^{\;1/2} / \omega_{FOV}^{\;1/2} \tag{5}$$

The instantaneous field-of-view is, in turn, related to the optics diameter, D, the system f-number, F, and the detector area A_d by

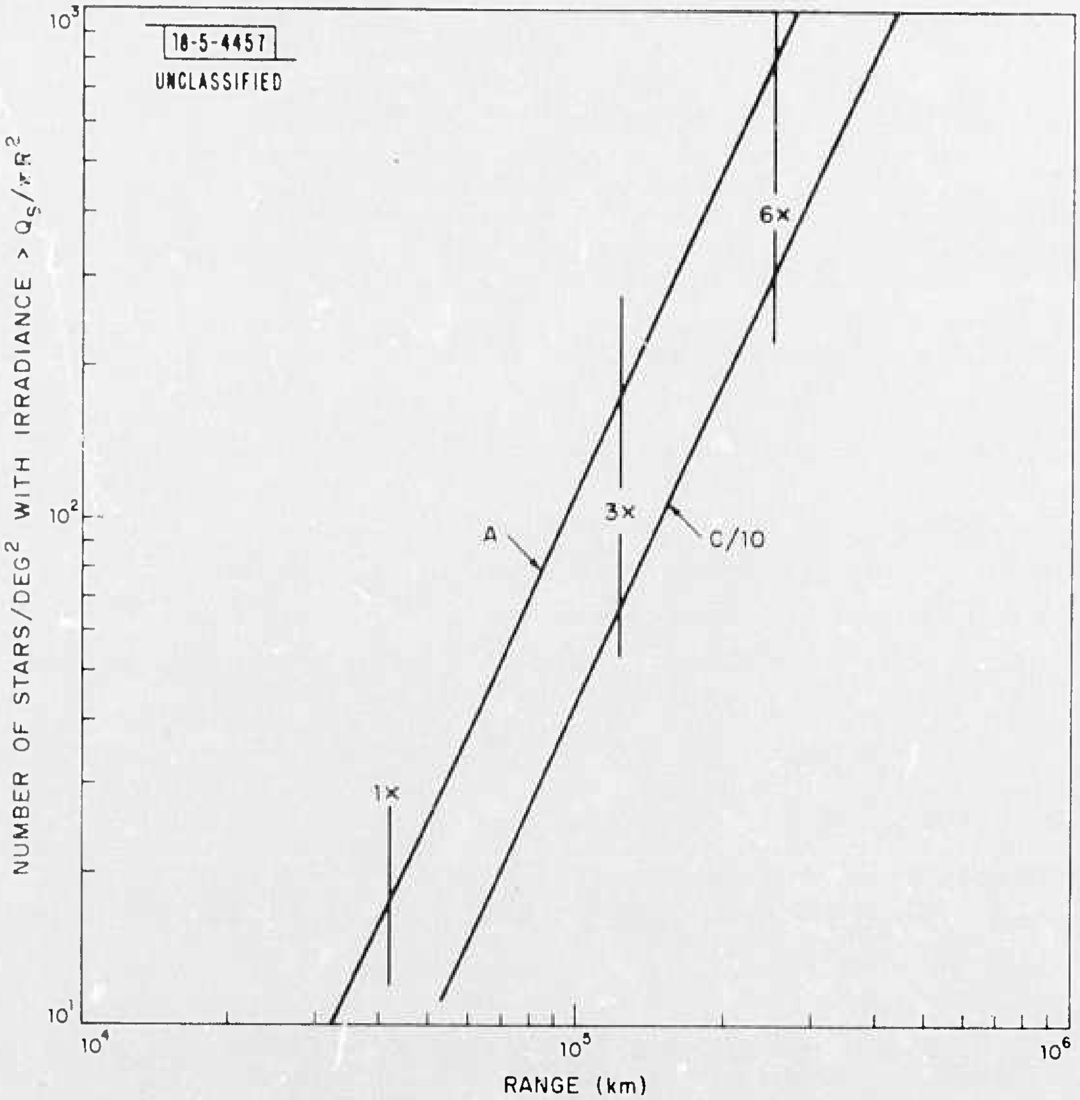

Fig. 3. Star background densities. (U)

$$\omega_{FOV} = \frac{A_d}{F^2 D^2} \tag{6}$$

Substituting in Eq. 4 we obtain

$$R^2 = \frac{Q_s \; D T_o}{4(SNR)}{}^{1/2} \; \Omega_{FOV}^{1/4} \; \dot{\Omega}^{-1/2} \left(\frac{2\eta DF}{Q_B A_d{}^{1/2}} \right)^{1/2} \tag{7}$$

(U) In the amplifier limit the range-sensitivity equation is given by Eq. A-45,

$$R^2 = \frac{Q_s h\nu \; D^2 T_o}{4(SNR) \; \overline{NEP}} \sqrt{8} \; (n\omega_{FOV} \dot{\Omega}^{-1}) \tag{8}$$

where $\overline{NEP}$ is a constant in the amplifier limit given by

$$\overline{NEP} = NEP \; (B/2)^{-1/2} \tag{9}$$

where NEP is the detector-amplifier noise-equivalent power and B is the system bandwidth. Substituting in Eq. 8 we obtain

$$R^2 = \frac{Q_s D T_o}{4(SNR)}{}^{1/2} \; \Omega_{FOV}{}^{1/4} \dot{\Omega}^{-1/2} \left(\frac{8(h\nu)^2 T_o \Omega_{FOV}{}^{1/2} A_d}{\overline{NEP}^2 \; F^2 \; \dot{\Omega}} \right)^{1/2} . \tag{10}$$

In actual operation, of course, both amplifier and background noise will be present in which case Eqs. (7) and (10) should be combined to give

$$R^2 = \frac{Q_s \; D T_o}{4(SNR)}{}^{1/2} \; \Omega_{FOV}{}^{1/4} \dot{\Omega}^{-1/2} \left\{ \frac{Q_B A_d{}^{1/2}}{2\eta DF} + \frac{\overline{NEP}^2 \cdot F^2 \cdot \dot{\Omega}}{8(h\nu)^2 T_o \Omega_{FOV}{}^{1/2} A_d} \right\}^{-1/2} . \tag{11}$$

Equation (11) reduces to Eq. (7) or Eq. (10) as Q_B or $\overline{NEP}$ is large. The range-sensitivity given by Eq. (11) can be maximized by selecting the optimum value of the detector area, A_d. This is given by differentiating Eq. (11) with respect to A_d and setting the result equal to zero. This gives

$$A_d^{3/2} = \frac{\overline{NEP}^2 \; F^3}{2(h\nu)^2 T_o} \cdot \frac{\eta D}{Q_B} \; \frac{\dot{\Omega}}{\Omega_{FOV}^{1/2}} , \qquad (12)$$

in which case Eq. (11) becomes

$$R^2 = \frac{Q_s}{2(SNR)} \left\{ \frac{\sqrt{2}}{\sqrt{27}} \; \frac{\eta \; T_o^2 \; \Omega_{FOV}}{Q_B \; \dot{\Omega}^2} \; \frac{h\nu}{\overline{NEP}} \; D^4 \right\}^{1/3} \qquad (13)$$

There are two constraints on this optimization: (1) A_d must be greater than or equal to the optics diffraction limit

$$A_d \geq (2.44 \; F\lambda)^2 , \qquad (14)$$

and, (2) A_d must be small enough to provide sufficient resolution to obtain good angular tracking accuracy and also to prevent a large number of the detectors from having a star in their field-of-view a large percentage of the time. Substitution of Eq. (14) in Eq. (12) results in the following constraint on the optics diameter

$$D \geq \frac{2(h\nu)^2 T_o}{\overline{NEP}^2} \; \frac{Q_B \Omega_{FOV}^{1/2}}{\eta \quad \dot{\Omega}} \; (2.44\lambda)^3 . \qquad (15)$$

The following parameter values are assumed:

$SNR = 7$

$\eta = 0.5$

$T_o = 0.5$

$\Omega_{FOV} = 0.04$ str. (0.2x0.2 radian)

$Q_B = 2.42 \times 10^{10}$ photons/sec cm^2

$\dot{\Omega} = 9.7 \times 10^{-4}$ str/sec = 3.5 str/hour

$\overline{NEP} = 5.4 \times 10^{-18}$ W/Hz (at 19μm)

$h\nu = 1.045 \times 10^{-20}$ W sec (at 19μm)

$\overline{NEP}/h\nu = 516.7$

The values are the same as assumed in the earlier study except for $\overline{NEP}$. The above value represents the best results obtained on a single detector rather than an average. It is assumed that in the future it will be possible to fabricate and assemble many detectors with this performance. There is some technical uncertainty in this.

(U) Substitution of these parameter values into Eq. (15) yields the constraint

$$D \geq 5.78\text{cm} = 2.28 \text{ inches} \tag{16}$$

All systems considered below satisfy this con traint. It is seen below also that the star occupancy (number of detectors which at any one instant in time have a star in their field-of-view with irradiance greater than or equal to that of the target sought) remains acceptable ($\lesssim$1%) for all systems considered.

(U) Using Eq. (13) we can calculate the optics diameter required to detect targets A and C/10 as a function of range. The results are shown in Fig. 4. The increase in spectral band from 8-14μm to 8-22μm along with the above optimization procedure has allowed a reduction in the optics diameter required to detect target C/10 at 3 times synchronous (3X) from 28 inches in the previous study to 19 inches. The approximate ranges to synchronous (1X), three times synchronous (3X) and six times synchronous (6X) altitude are indicated in the figure. The 6x altitude is assumed to be about the limit of sublunar stable orbits.

(U) The star occupancy, ε, can be calculated from

$$\varepsilon = \omega_{FOV} \cdot N \tag{17}$$

where N is the number of stars/deg^2 given in Fig. 3 if ω_{FOV} is in deg^2. The star occupancy for targets A and C/10 is shown in Fig. 5 for the linear array from Eq. (17). As can be seen from Fig. 5 the star occupancies all lie below about 1% which is

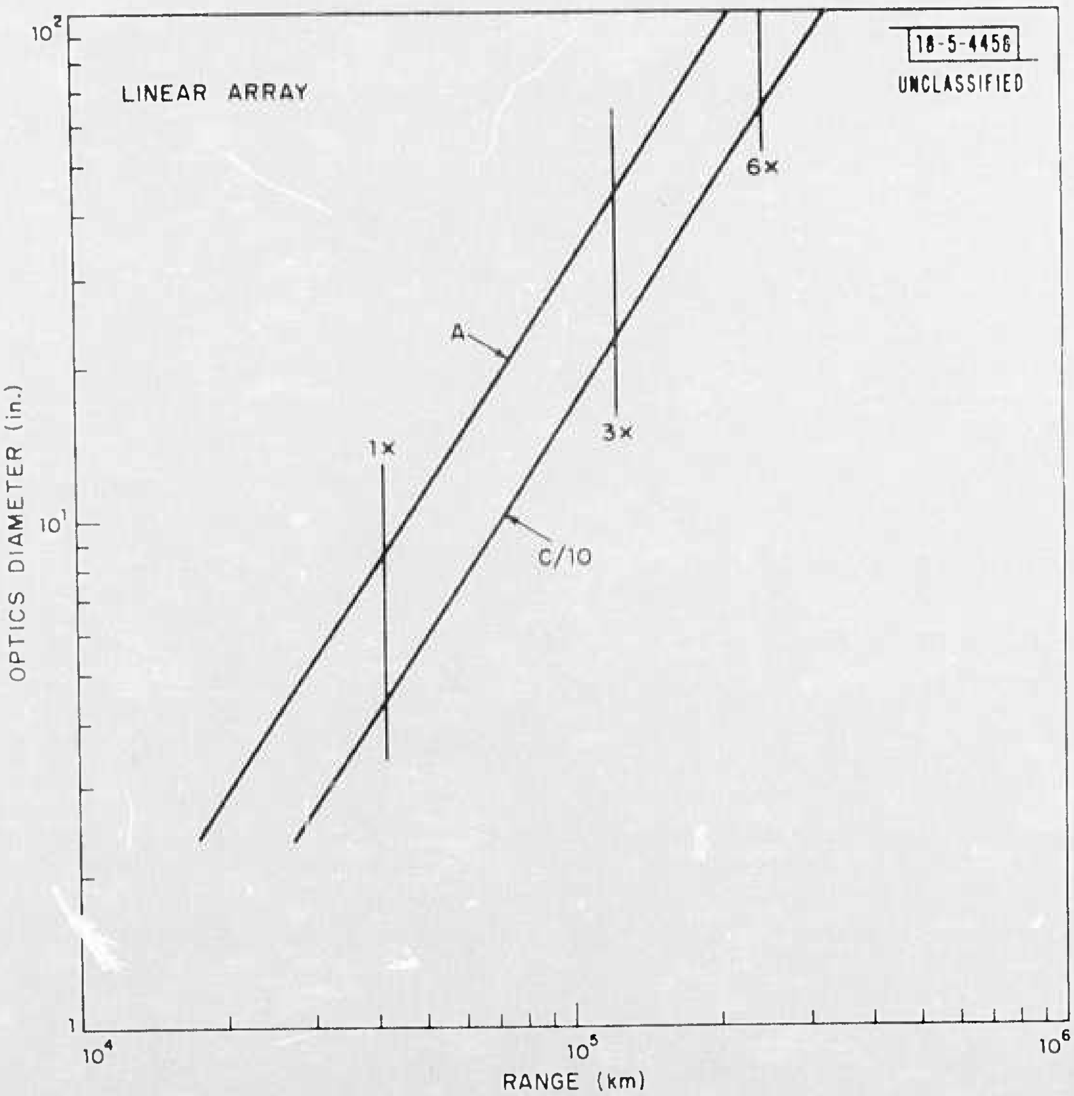

Fig. 4. Linear array optics diameter. (U)

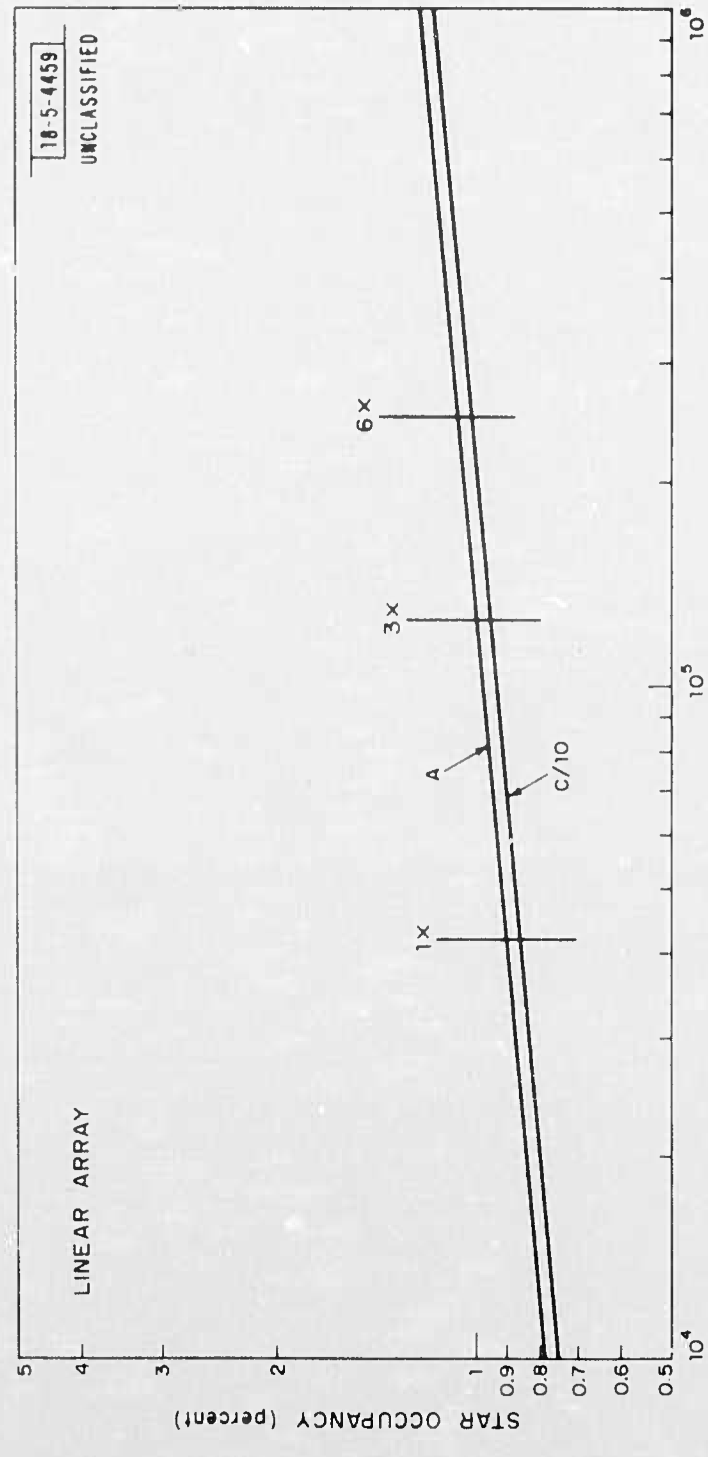

Fig. 5. Linear array star occupancy. (U)

deemed very acceptable. The linear array detector element size for an arbitrary F/3 system is shown vs. range for the three targets in Fig. 6. The f-number is not an important parameter in this analysis and F/3 was selected as it appears reasonable to expect that the optical systems could be built with the required resolution at F/3. The last parameter of importance in the linear array is the number of individual detectors required. This is given by Eq.(5) and is plotted vs. range for targets A and C/10 in Fig. 7. The number used for target C/10 at 3X range is 780 vs. 500 assumed in the earlier study. This is a result of the optimization process and is partly responsible for the reduction in required optics diameter. As in the earlier study we assume two rows of detectors in order to provide star discrimination. Thus the total number of detectors is twice the number given in Fig. 7.

(U) The vidicon analysis proceeds in a manner similar to the discussion of Appendix A of the earlier study report. From Eq. A-55 therein we have

$$R^2 = \frac{Q_S}{2(SNR)} D\left(\frac{T_o \quad \eta G m \; n t_F}{Q_B \quad \Omega_{FOV}}\right)^{1/2} \tag{18}$$

where η is the quantum efficiency and G the photoconductive gain of the vidicon retina, m is a modulation index characteristic of the readout mechanism, n is the total number of resolution elements, t_F is the frame time and Ω_{FOV} is the total vidicon instantaneous field-of-view. The range-sensitivity is maximized when the system is diffraction limited in which case

$$n = \Omega_{FOV}/\omega_{FOV} = \Omega_{FOV}/(2.44\lambda/D)^2. \tag{19}$$

The frame time allowed is limited by the length of time the target image remains focussed on a single resolution element. If α is the angular rate of target motion with respect to the sensor

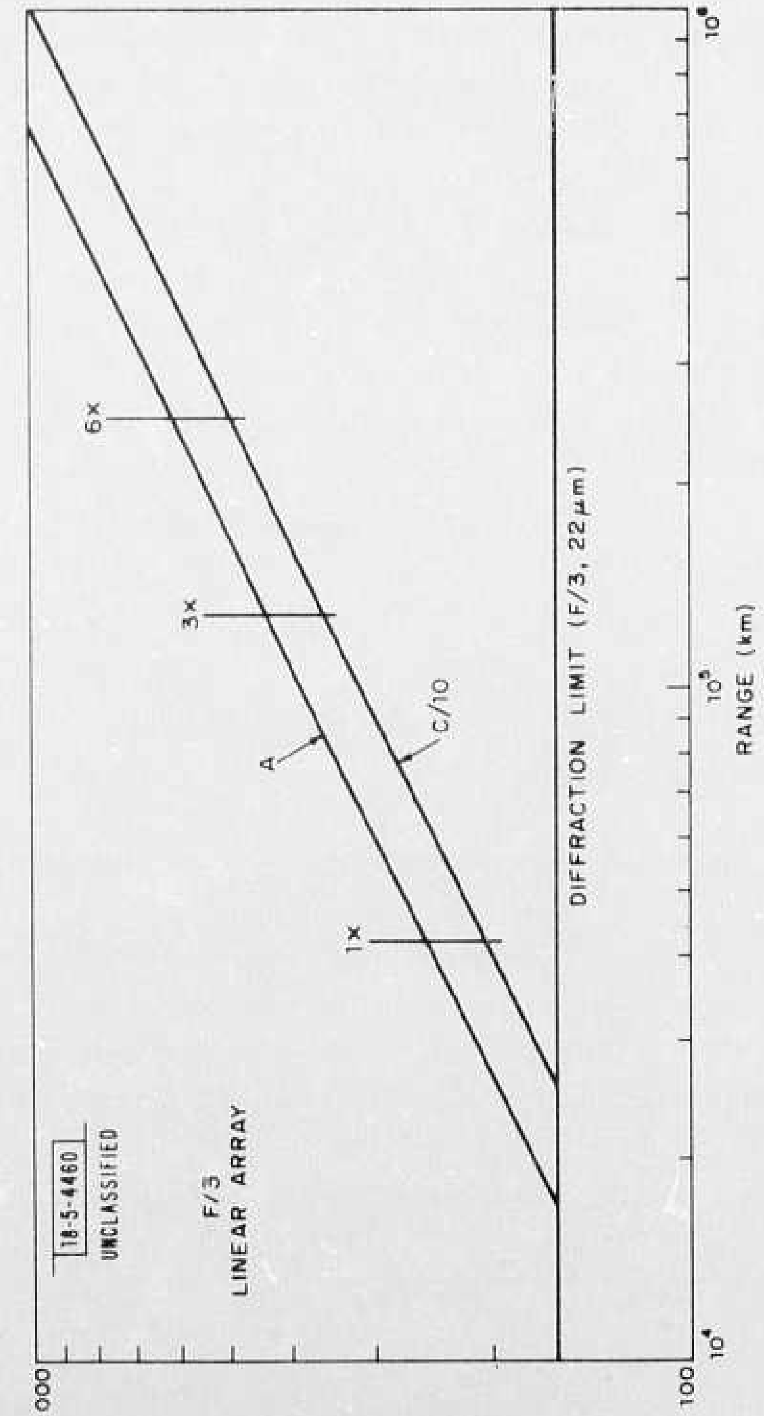

Fig. 6. Linear array detector element size. (U)

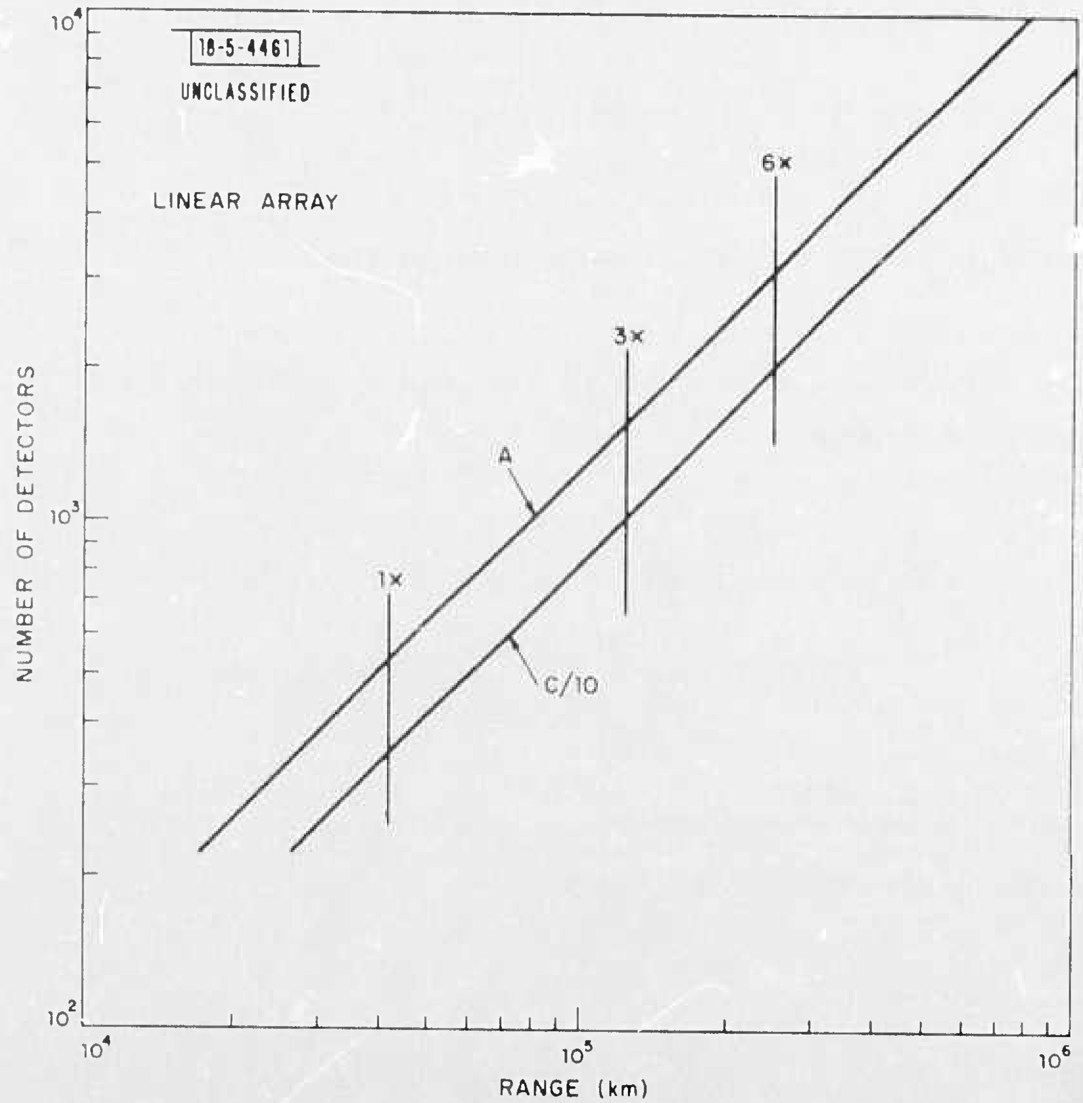

Fig. 7. Single linear array number of detector elements. (U)

line-of-sight which is assumed fixed in inertial space then the frame time is limited by

$$t_F \leq \frac{\omega_{FOV}^{1/2}}{\alpha} = \frac{2.44\lambda}{\alpha D} \qquad (20)$$

For the moment we will assume

$$t_F = \frac{2.44\lambda}{\alpha D} \quad . \qquad (21)$$

The angular rate of target motion is given by

$$\alpha = V/R \qquad (22)$$

where V is the relative velocities of the target and sensor satellites perpendicular to the line of sight and R is the sensor-to-target range. For a high-orbit target and a lower orbit sensor satellite, V will be dominated by the sensor motion. Substituting Eqs. (19), (21) and (22) in Eq. (18) we obtain

$$R^{3/2} = \frac{Q_s}{2(SNR)} \; D^{3/2} \left(\frac{T_o \; \eta G m}{Q_B \cdot 2.44\lambda \cdot V} \right)^{1/2} \qquad (23)$$

and

$$t_F = \frac{2.44\lambda R}{V \cdot D} \qquad (24)$$

The new parameters assumed are

$\eta = 0.5$

$G = 0.5$

$m = 1/4$

$V = 3$km/sec (Synchronous Orbital Velocity).

These values are about the same as those assumed in the previous study except for the modulation index. We are assuming for the present study a photoconductive vidicon with an "Isocon" read-out. The theoretical best modulation index for such a device is m=1/2. However, assessment of practically achievable isocon performances indicates a factor of about 2 degradation below theoretical leading to the assumed value of m=1/4. This is also approximately borne out by theoretical analysis of the tube performance. Using Eq.(23) and (24) we obtain the following frame time

$$t_F = 11.6 \text{ sec} \tag{25}$$

Equation (23) can be used to evaluate the optics diameter necessary to see targets A, and C/10. The result of this is shown in Fig. 8 vs. sensor-to-target range. The decrease in required optics diameter for target C/10 at 3X range from 6 1/2" in the earlier study to 4 1/2" is due primarily to the increase in spectral bandwidth employed. The star occupancy for the vidicon can be calculated using Eq.(19) and

$$\omega_{FOV} = \left(\frac{2.44\lambda}{D}\right)^2, \tag{26}$$

the diffraction limit. The results are included in Fig. 9. The approximate 5% occupancy factor, although larger than for the linear array, is close to that imposed on the other optical systems.

(U) Since the vidicon is assumed to operate at a constant frame rate the required field-of-view is

$$\Omega_{FOV} = \dot{\Omega}\ t_F\ . \tag{27}$$

For a scan rate of 4 str/hour and t_F given by Eq. (25)

$$\Omega_{FOV}^{1/2} = 0.11 \text{ radian} = 6.5° \tag{28}$$

(U) A direct comparison between the linear array and the vidicon required optics diameter is shown in Fig. 10. As can be seen the vidicon system requires considerably less optical diameter at all ranges especially for the more distant targets.

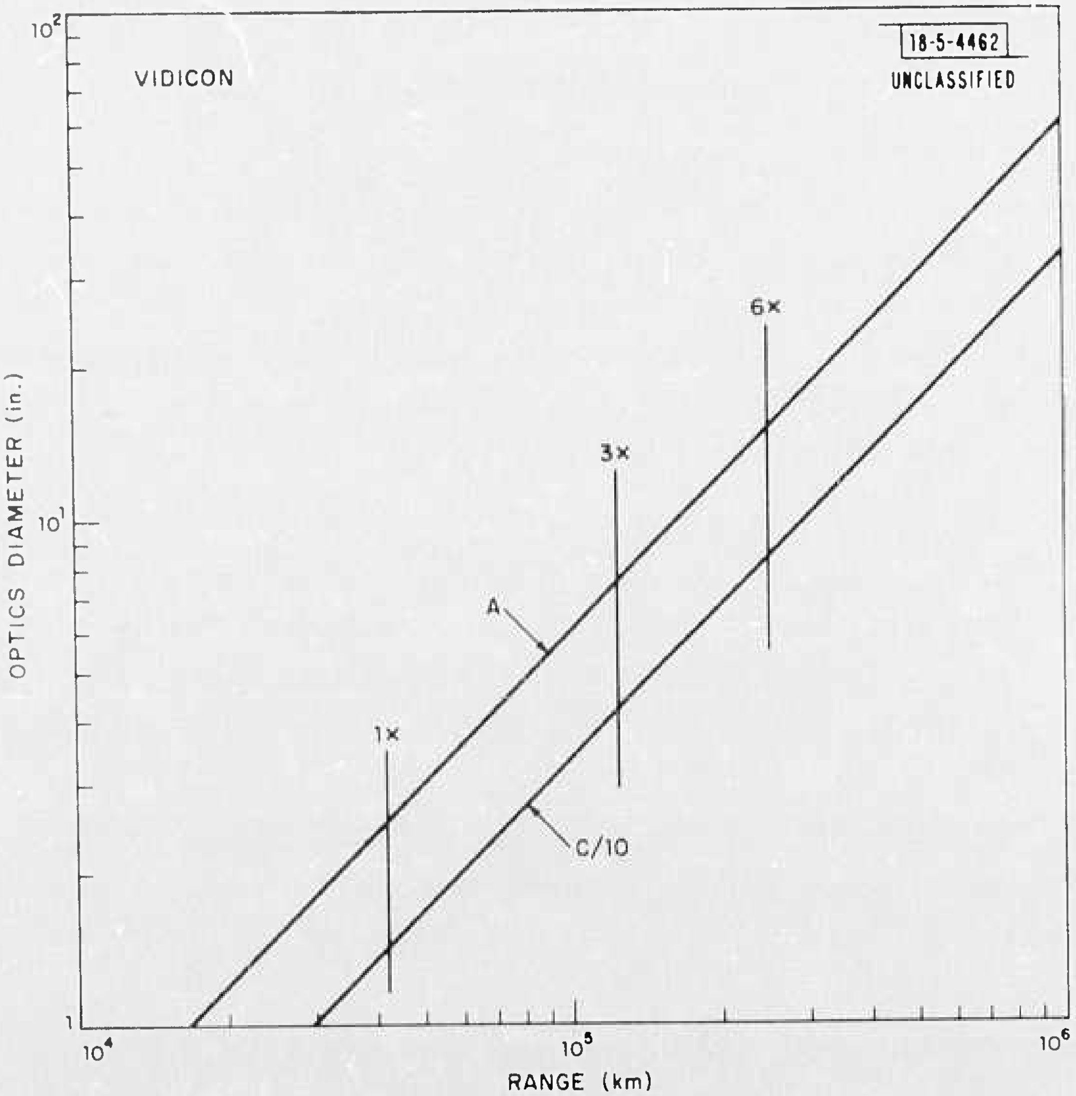

Fig. 8. Vidicon optics diameter. (U)

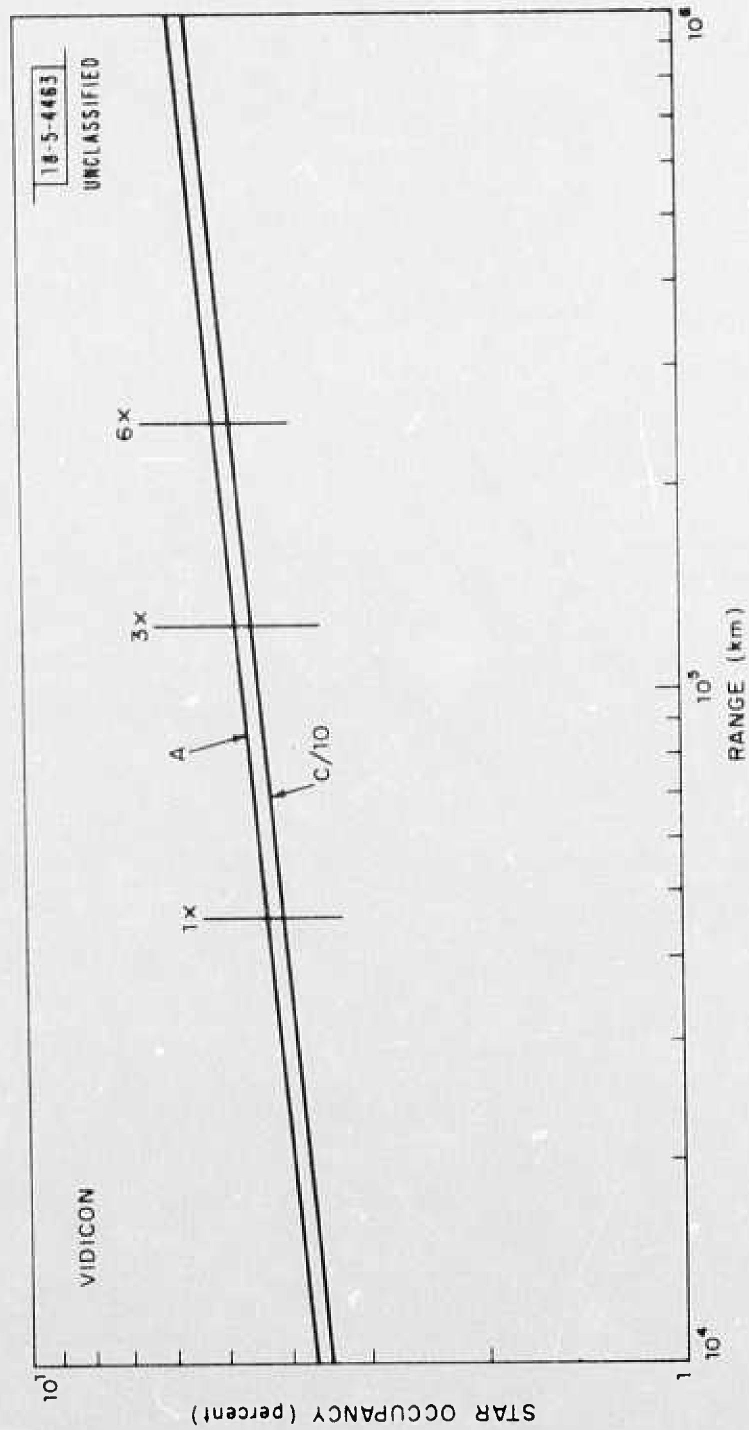

Fig. 9. Vidicon star occupancy. (U)

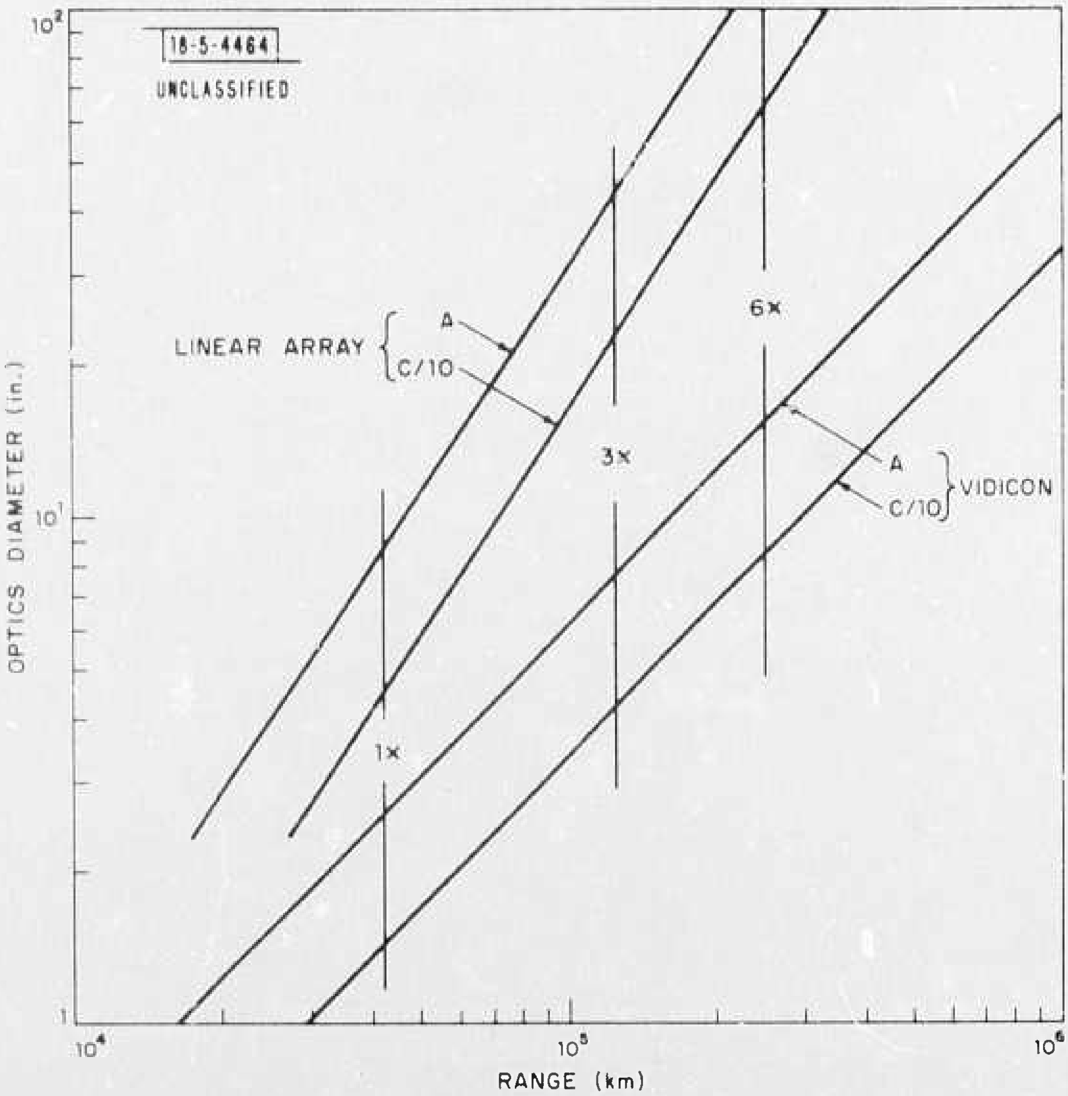

Fig. 10. Linear array and vidicon optics diameter comparison. (U)

REFERENCES

1. Project Report PSI-3, "Satellite Surveillance with Optical Satellites" (U), Lincoln Laboratory, M.I.T. (15 August 1972), SECRET.

2. B. T. Soifer, J. R. Houck and M. Harwit, "Rocket Infrared Observations of the Interplanetary Medium," Astrophys. J. 168, L73 (1971).

3. S. D. Price and R. G. Walker, "Further Results from Hi Star (U)," Minutes of the Fifteenth Midcourse Measurements Meeting, May 1972, SECRET.

4. Final Report, "Spacetrack Augmentation Study I, Vol. I and II (U)," Philco-Ford Corporation, Aeronutronic Division, Newport Beach, California SAMSO-TR-72-160, SECRET.

UNCLASSIFIED

Security Classification

SECRET

DOCUMENT CONTROL DATA – R&D

(Security classification of title, body of abstract and indexing annotation must be entered when the overall report is classified)

1. ORIGINATING ACTIVITY *(Corporate author)* Lincoln Laboratory, M.I.T.	2a. REPORT SECURITY CLASSIFICATION SECRET	
	2b. GROUP XLGDS-3	
3. REPORT TITLE IR Satellite Surveillance		
4. DESCRIPTIVE NOTES *(Type of report and inclusive dates)* Technical Note		
5. AUTHOR(S) *(Last name, first name, initial)* Dimmock, John O.		
6. REPORT DATE 2 May 1973	7a. TOTAL NO. OF PAGES 26	7b. NO. OF REFS 4
8a. CONTRACT OR GRANT NO. F19628-73-C-0002	9a. ORIGINATOR'S REPORT NUMBER(S) Technical Note 1973-19	
b. PROJECT NO. ARPA Order 600	9b. OTHER REPORT NO(S) *(Any other numbers that may be assigned this report)* ESD-TR-73-99	
c.		
d.		
10. AVAILABILITY/LIMITATION NOTICES Distribution limited to U.S. Government agencies only; test and evaluation; 11 May 1973. Other requests for this document must be referred to ESD-DR-2.		
11. SUPPLEMENTARY NOTES None	12. SPONSORING MILITARY ACTIVITY Advanced Research Projects Agency, Department of Defense	

13. ABSTRACT

A calculation and a comparison is made between the capabilities of a linear array of infrared detectors and those of an infrared vidicon for detecting high-altitude satellites from a satellite sensor platform. It is shown that far smaller optics diameter is required for the vidicon sensor to achieve the same range as the linear array or alternatively the vidicon range is far greater.

14. KEY WORDS

IR detectors	vidicon sensor
satellite surveillance	linear array

SECRET

pl1-1800

UNCLASSIFIED

Security Classification

(This page is unclassified)

UNCLASSIFIED

AD 525 790

CLASSIFICATION CHANGED

TO: UNCLASSIFIED

FROM: SECRET

AUTHORITY: DARPA ltr, 26 Oct 83

UNCLASSIFIED